IMMUNOBIOLOGY

Forced miR-146a expression causes autoimmune lymphoproliferative syndrome in mice via downregulation of Fas in germinal center B cells

Qiuye Guo,[1,2] Jinjun Zhang,[1] Jingyi Li,[1,3] Liyun Zou,[1] Jinyu Zhang,[1] Zunyi Xie,[1] Xiaolan Fu,[1] Shan Jiang,[4] Gang Chen,[5] Qingzhu Jia,[5] Fei Li,[5] Ying Wan,[5] and Yuzhang Wu[1]

[1]Institute of Immunology, People's Liberation Army, Third Military Medical University, Chongqing, China; [2]Institute of Genetic Engineering, Southern Medical University, Guangzhou, China; [3]Department of Rheumatology, Southwest Hospital, Third Military Medical University, Chongqing, China; [4]Department of Immunology, Duke University Medical Center, Durham, NC; and [5]Biomedical Analysis Center, Third Military Medical University, Chongqing, China

Key Points

- miR-146a may be involved in the pathogenesis of ALPS by targeting Fas.
- Sustained expression of miR-146a in B cells is the major factor leading to the enhanced homeostatic expansion of B and T cells.

By inhibiting target gene expression, microRNAs (miRNAs) play major roles in various physiological and pathological processes. miR-146a, a miRNA induced upon lipopolysaccharide (LPS) stimulation and virus infection, is also highly expressed in patients with immune disorders such as rheumatoid arthritis, Sjögren's syndrome, and psoriasis. Whether the high level of miR-146a contributes to any of these pathogenesis-related processes remains unknown. To elucidate the function of miR-146a in vivo, we generated a transgenic (TG) mouse line overexpressing miR-146a. Starting at an early age, these TG mice developed spontaneous immune disorders that mimicked human autoimmune lymphoproliferative syndrome (ALPS) with distinct manifestations, including enlarged spleens and lymph nodes, inflammatory infiltration in the livers and lungs, increased levels of double-negative T cells in peripheral blood, and increased serum immunoglobulin G levels. Moreover, with the adoptive transfer approach, we found that the B-cell population was the major etiological factor and that the expression of Fas, a direct target of miR-146a, was significantly dampened in TG germinal center B cells. These results indicate that miR-146a may be involved in the pathogenesis of ALPS by targeting Fas and may therefore serve as a novel therapeutic target. (*Blood*. 2013;121(24):4875-4883)

Introduction

MicroRNAs (miRNAs) are a new class of RNA molecules that play an important role in posttranscriptional gene regulation. Bioinformatic analysis has estimated that the mammalian miRNA repertoire may directly regulate up to 30% of all protein-encoding genes.[1] Changes in hundreds of proteins due to miRNA repression can be detected by a quantitative proteomics approach.[2] In recent years, rapidly accumulating evidence has demonstrated that miRNAs are key players in diverse physiological and pathophysiological processes.[1,3] Therefore, it is not surprising that miRNAs act as indispensable fine-tuners for the regulation of endogenous gene expression in immune homeostasis.[4-6]

Among the functionally evaluated miRNAs, miR-146a was the first to be reported as a key factor modulating the innate immune response. Upon lipopolysaccharide (LPS) stimulation and virus infection, miR-146a acts as a negative feedback regulator and restrains the Toll-like receptor signaling pathways by targeting IRAK1/2 and TRAF6 in various innate cells such as monocytes, lung epithelial alveolar cells, and microglial cells.[7-10] In the adoptive immune system, miR-146a has previously been reported to target Fas-Associated protein with Death Domain to modulate activation-induced cell death and interleukin-2 (IL-2) expression in Jurkat T cells.[11] Ablation of miR-146a in mice leads to increased numbers of Treg cells but impairs their suppressor function because of the unrestrained function of STAT1.[12] These studies suggest that miR-146a functions as a robust "brake" during the inflammation and adoptive immune responses.

miRNA-expression profiling has shown that miR-146a levels are dynamically regulated during the physiological and pathological immune responses. In comparison with naive B or T lymphocytes, miR-146a is much more abundant in various differentiated lymphocyte subsets such as Tfh, Treg, and germinal center (GC) B cells.[13] In addition, our previous data showed that miR-146a expression levels were significantly elevated in the $CD4^+$ T cells of rheumatoid arthritis patients and that this elevation was closely associated with the serum tumor necrosis factor-α level.[14] This expression pattern is not restricted to rheumatoid arthritis, and similar results have been noted in patients with cancers or autoimmune disorders, including Sjögren's syndrome and psoriasis.[15-21] miR-146a accumulation in these inflammatory or autoimmune conditions cannot explain or be explained by its immunosuppressive nature in innate cells.

To investigate the potential pathological roles of accumulated miR-146a in vivo, we developed a transgenic (TG) mouse strain constitutively expressing miR-146a. When there was a threefold to

Submitted August 29, 2012; accepted April 16, 2013. Prepublished online as *Blood* First Edition paper, May 3, 2013; DOI 10.1182/blood-2012-08-452425.

Q.G., J.Z., and J.L. contributed equally to the work and are the co-first authors of this paper.

The online version of this article contains a data supplement.

The publication costs of this article were defrayed in part by page charge payment. Therefore, and solely to indicate this fact, this article is hereby marked "advertisement" in accordance with 18 USC section 1734.

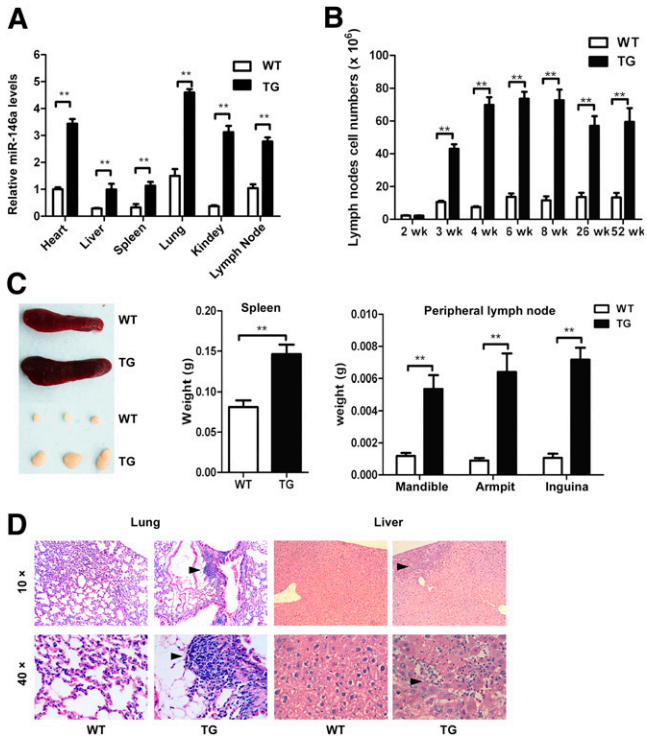

Figure 1. Generation of miR-146a-overexpressing TG mice. (A) qRT-PCR analysis of mature miR-146a expression in various tissues from WT and TG mice. The miR-146a expression levels from different tissues were normalized to the snoRNA-135 level. (B) Cell counts of 8 pLNs (2 from the mandible, 4 from the armpit, 2 from the inguina of mice, at age 2–6 weeks [n = 4]). (C) Splenomegaly and lymphadenopathy in TG mice. The photographs show the spleens (left top) and peripheral lymph nodes (left bottom) from representative mice at age 8 weeks. The weights of spleen (middle; n = 7) and peripheral lymph nodes (right; n = 7; from the mandible, the armpit, and the inguina of the mice) were measured. (D) Mixed cellular inflammatory infiltrations (arrowheads) in hematoxylin-eosin–stained sections of the lungs and livers from 8-week-old TG and WT mice (top, low magnification; bottom, high magnification). All data are expressed in terms of mean ± standard deviation values. Comparison of means was performed with an unpaired Student 2-tailed *t* test (**$P < .01$).

eightfold increase in miR-146a expression, which is reminiscent of that found in patients, the TG mice spontaneously developed immune symptoms remarkably similar to the manifestations of autoimmune lymphoproliferative syndrome (ALPS). Further cellular and molecular analyses suggested that Fas suppression by miR-146a represents a major etiological factor for these pathological manifestations.

Methods

Generation of miR-146a TG mice

A lentivirus vector (FUGW-miR146a) with a ubiquitin promoter and a green fluorescent protein (GFP) reporter gene[14] was prepared using calcium phosphate precipitation and concentrated with centrifugation at 50 000 × *g* for 2 hours. The concentrated virus suspension (1×10^9 transducing units/mL) was injected into the perivitelline space of single-cell embryos from BALB/c mice as described in a previous study.[22] The miR-146a and miR-146a* expressions in TG mice were analyzed using real-time reverse-transcription polymerase chain reaction (RT-PCR) based on the manufacturer's protocols (TaqMan MicroRNA Transcription Kits, TaqMan MicroRNA Assay, and TaqMan Universal Master Mixes II; Applied Biosystems). The miR-146a and miR-146a* expression levels from different tissues were normalized to the snoRNA-135 level. Data were analyzed with the $2^{(-\Delta\Delta CT)}$ method.[23] All the mice were bred and maintained under specific pathogen-free conditions at the Center of Laboratory Animals of the Third Military Medical University. Animal maintenance and experimental procedures were carried out in accordance with the National Institutes of Health Guidelines for the Use of Experimental Animals and were approved by the Medicine Animal Care Committee of the Third Military Medical University (Chongqing, China).

Pathological and immunochemistry analyses

Organs, including the heart, liver, lung, kidney, spleen, and lymph nodes, were removed from mice and placed immediately in 4% formalin. Samples were stained with hematoxylin and eosin. GCs were stained with peanut agglutinin (PNA; Sigma-Aldrich) and biotinylated anti-PNA antibody (Vector Laboratories, Inc.).

Immunoglobulin isotyping analysis

Sera (1: 25 000) were used for immunoglobulin isotyping via a bead-based multiplex luminex assay (MILLIPLEX MAP Mouse Immunoglobulin Isotyping; Millipore, Billerica, MA).

Flow cytometry

Cells were harvested from various lymphoid organs, including peripheral lymph nodes (pLNs), mediastinal lymph nodes (mLNs), and Peyer's patches (PPs). Single-cell suspensions were prepared in precooled phosphate-buffered saline with 5% fetal bovine serum and stained with anti-CD95/Fas (clone 15A7), anti-CD38 (clone 90), anti-CD19 (eBio1D3), anti-CD3 (clone 17A2), anti-CD4 (clone RM4-5), anti-CD8a (clone 53-6.7), anti-CD4 (clone GK1.5), anti-CD44 (clone IM7), anti-CD62L (clone MEL-14), anti-CD25 (clone PC61.5), anti-CD69 (clone H1.2F3), and anti-B220/CD45R (clone RA3-6B2) (eBioscience). GCs were stained with peanut agglutinin (PNA; Sigma-Aldrich). Affinity-purified anti-mouse CD16/32 antibody (eBioscience) was used to block the Fc receptors. All samples were analyzed using FACSAria I (BD Biosciences), and the data were analyzed with the FlowJo software (Tree Star, Inc.).

Adoptive transfers

Non-GC B ($CD19^+CD38^{high}Fas^-$) cells from the wild-type (WT) and miR-146a TG mice were sorted using the FACSAria II. B cells or $CD4^+$ T cells were isolated from lymph nodes with an untouched isolation strategy (B Cell Isolation Kit and $CD4^+$ T Cell Isolation Kit II; Miltenyi Biotec). Dead cells were removed with the Dead Cell Removal Kit (Miltenyi Biotec). For analysis of the GC B population after adoptive transfer, non-GC B cells (1×10^6) mixed with WT $CD4^+$ T cells (1×10^6) in a 1:1 ratio were adoptively transferred into BABL/c SCID recipient mice through intravenous injection. For the homeostasis proliferation assay, isolated B cells (1×10^6) or $CD4^+$ T cells (1×10^6) were adoptively transferred into SCID mice. Lymphocytes from the donor mice were analyzed within the spleens of recipient mice by fluorescence-activated cell sorter (FACS) at 7 days after adoptive transfer.

Cell proliferation analysis

To detect homeostasis proliferation of lymphocytes, SCID mice were administered 200 μL of EdU (500 μg/mL) by intraperitoneal injections at 24 hours after adoptive transfer. EdU was administered twice within a 48-hour interval. The recipient mice were sacrificed 7 days after adoptive transfer. Accumulation of EdU incorporation in splenic lymphocytes was analyzed by FACS (Click-iT EdU Cell Proliferation Assays; Invitrogen). The in vitro B-cell proliferation assay was performed as follows. The isolated B cells were labeled with 5 μM Cell Proliferation Dye eFluor 670 (an alternative cell proliferation dye of carboxyfluorescein diacetate succinimidyl ester [CFSE]; eBioscience) for 5 minutes. The labeled B cells (1×10^6) were stimulated with 0.1 μg/mL LPS in complete RPMI1640 for 3 days in 96-well plates. The cells were then harvested and analyzed by FACS.

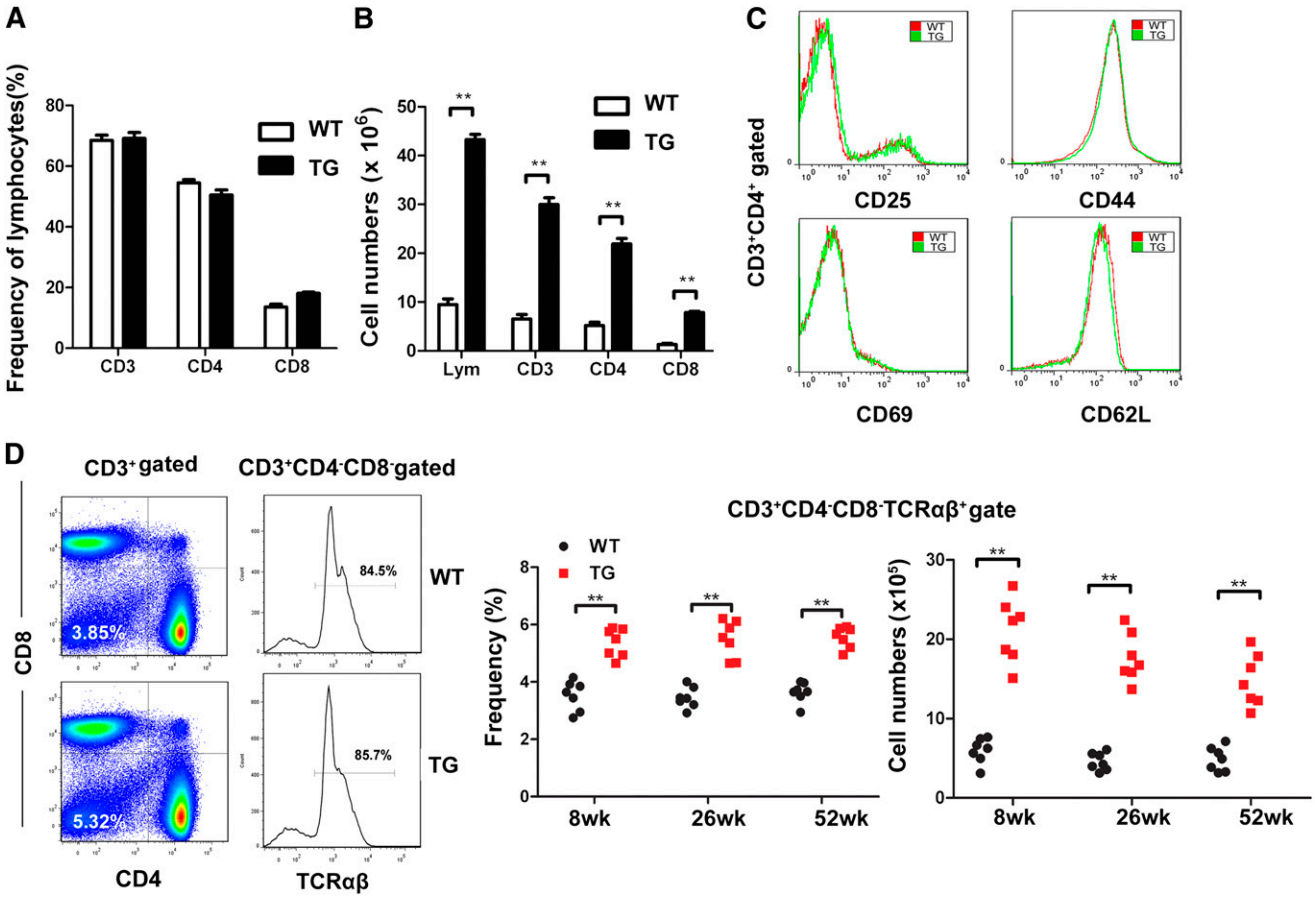

Figure 2. DN T cells are significantly increased in peripheral lymphoid organs. (A) The frequency of T-lymphocyte subsets in dLNs from WT and miR-146a TG mice at age 6 to 8 weeks. (B) The T-cell numbers of indicated lymphocyte subsets in dLNs (n = 4). (C) The expression of activation markers on $CD4^+$ T cells from peripheral LNs by FACS analysis. (D) Increased $CD3^+CD4^-CD8^-TCR\alpha\beta^+$ DN T cells in the spleens from TG mice. Both the frequency and cell numbers were increased significantly in TG mice from 8 to 52 weeks. Results shown here are representative of at least 3 independent experiments (WT, n = 5; TG, n = 6). All data are expressed in terms of mean ± standard deviation values. Comparison of means was performed with an unpaired Student 2-tailed *t* test (**$P < .01$).

Luciferase reporter assay

The vector containing the 3′-untranslated region (UTR) of Fas (pEZX-Luc-Fas) together with a plasmid encoding either miR-146a (pEZX-miR-146) or miR-scramble (pEZX-miR-scramble) were cotransfected into 293FT cells with Lipofection 2000 (Invitrogen). All the vectors were acquired from GeneCopoeia. The luciferase assay was performed using the Dual-Luciferase Reporter Assay Kit (Promega) as previously described.[24]

Microarray analysis

B cells of the WT and miR-146a TG mice were isolated from lymph nodes with an untouched magnetic separated assay, and dead cells were depleted with the Dead Cell Removal Kit (Miltenyi Biotec). The cells were lysed with TRIzol reagent (Invitrogen). The upper phase containing the RNA (final ethanol concentration of 35%) was transferred to an RNeasy spin cartridge following the manufacturer's guide (Qiagen). Transcription profiles of the B cells were determined using Affymetrix MG 430 PM version chips (Affymetrix) according to the manufacturer's guide for cDNA synthesis, production of biotin-labeled cRNA, hybridization of cRNA to the chips, and scanning. Raw expression CEL files were processed with the Partek Express Affymetrix Edition software. Each probe ID of a mouse transcript was ranked by fold changes from up- to downregulation compared with that in WT controls. Sylamer miRNA seed enrichment analysis was performed using Markov correction.[25] The complete dataset from this analysis is available at the NCBI Gene Expression Omnibus, under accession no. GSE39779. All the values have been expressed in terms of mean ± standard deviation values. Comparison of means was performed with an unpaired Student 2-tailed *t* test, and statistical significance was accepted at *$P < .05$ and **$P < .01$.

Results

Generation of miR-146a TG mice

To investigate the pathogenic roles of miR-146a, concentrated lentivirus was microinjected, as described previously,[22] into the perivitelline space of single-cell embryos to generate mouse strains carrying the *mmu-miR-146a* transgene. Four of 7 (57%) founder animals expressed GFP at detectable levels by FACS. The founders were backcrossed with BALB/c mice for more than 9 generations. Since the genomic DNA fragment encoding miR-146a was preceded by a ubiquitin promoter and GFP in the vector FUGW-miR146a (supplemental Figure 1), a convenient approach was established for screening out TG mice with higher miR-146a expressions by detecting the GFP expression level in peripheral blood mononuclear cells (supplemental Figure 1). The expression levels of miR-146a were quantified by real-time PCR. The data showed threefold to eightfold forced expression in TG mice, and the levels varied among hearts, livers, spleens, lungs, kidneys, and lymph nodes (Figure 1A). The expression level of miR-146a coincidently matched that in

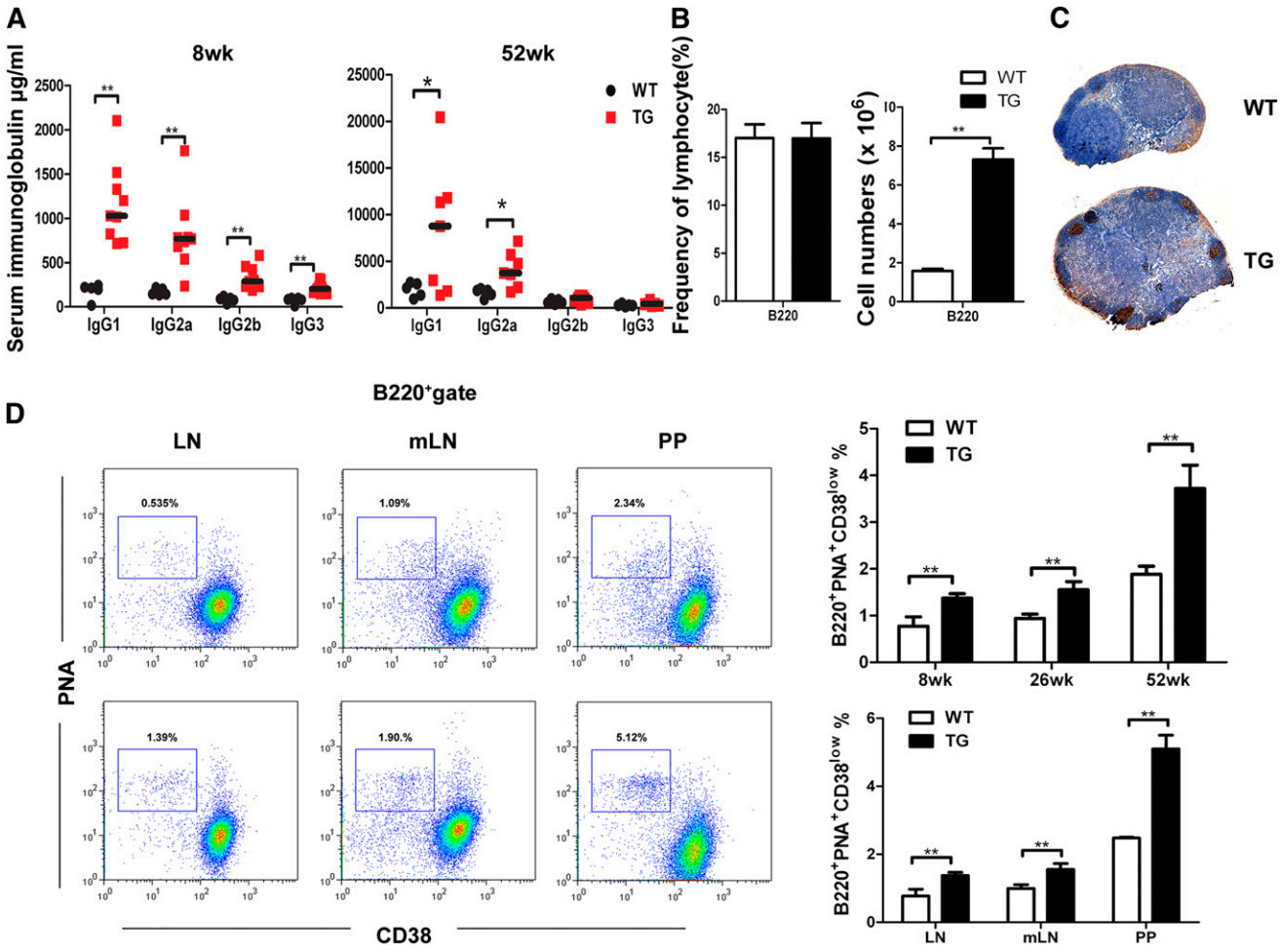

Figure 3. Accumulation of GC B cells, increased serum IgG levels, and spontaneous GC formation in miR-146a TG mice at early ages. (A) The immunoglobulin levels were measured by the Milliplex assay in the sera from TG (n = 7 - 9) and WT (n = 5) mice at age 8 and 52 weeks. (B) The B-cell frequency and numbers in dLNs from 6- to 8-week-old WT and TG mice. (C) Detection of GCs by the immunohistochemistry analysis on dLN sections from WT and TG mice (PNA, brown; hematoxylin, blue). (D) The percentage of $B220^+PNA^+CD38^{low}$GC B cells was determined by FACS in peripheral LNs from 8-, 26-, and 52-week-old mice, as well as in mLNs and PPs from 8-week-old mice (n = 4). All data are expressed in terms of mean ± standard deviation values. Comparison of means was performed with an unpaired Student 2-tailed *t* test. All data are representative of at least 3 independent experiments (*$P < .05$, **$P < .01$).

patients with autoimmune disorders.[16-18] Theoretically, in addition to miR-146a, our TG construct could produce mature miR-146a*. Although some star strand of miRNAs could be stable, our data indicated that this is not the case for miR-146a*. We measured the expression of miR-146a* and miR-146a using quantitative RT-PCR (TaqMan platform). Normalized to an endogenous control, snoRNA-135, we found that there is at least a 1700-fold difference in concentration between miR-146a and miR-146a* (supplemental Table 1). At such a low level of concentration, it is unlikely that miR-146a* can make any contribution to the phenotype observed in our TG mice. Our approach for generating TG mice with high miRNA expression is feasible for studying miR-146a function in immune disorders and may therefore be applied to extensive investigation of miRNA functions in vivo.

miR-146a TG mice developed pathological manifestations that mimic ALPS

Starting at age 3 weeks, miR-146a TG mice exhibited greatly enlarged spleens and lymph nodes (Figure 1C). Especially in the lymph nodes, the cellularity was threefold higher in TG animals at week 3, peaked to eightfold at week 4, and was maintained at fourfold from week 6 (Figure 1B). Except for monocyte counts, the hematological analysis showed no significant differences in white and red blood cell counts, red blood cell width distribution, mean corpuscular volume, lymphocyte count, hematocrit, hemoglobin level, or platelet production between the WT and TG mice at the age of 8 weeks (n = 10; supplemental Figure 2). In addition, the histopathological analysis also showed inflammation infiltrates in the lungs and livers of TG mice at age 8 weeks (Figure 1D).

We examined various subsets of lymphocytes in the lymph organs of miR-146a TG mice. Thymocyte development in TG mice was largely normal (supplemental Figure 3). While there was no significant change in the frequency of lymphocyte subsets compared with that in WT mice (Figure 2A), the numbers of $CD4^+$ and $CD8^+$ T cells were increased greatly due to the dramatic increase in cellularity (Figure 2B). Previous studies have suggested that miR-146a is involved in T-cell activation and Treg cell function.[11] In miR-146a TG mice, a slight decrease in Treg-cell frequency was observed (supplemental Figure 4). The spontaneous T-cell activation was assessed with surface markers, including CD25, CD69, CD44, and CD62L. No obvious activation was observed for either $CD4^+$ (Figure 2C) or $CD8^+$ T cells (data not shown), which suggested that the reduced frequency of Treg cells was not sufficient to

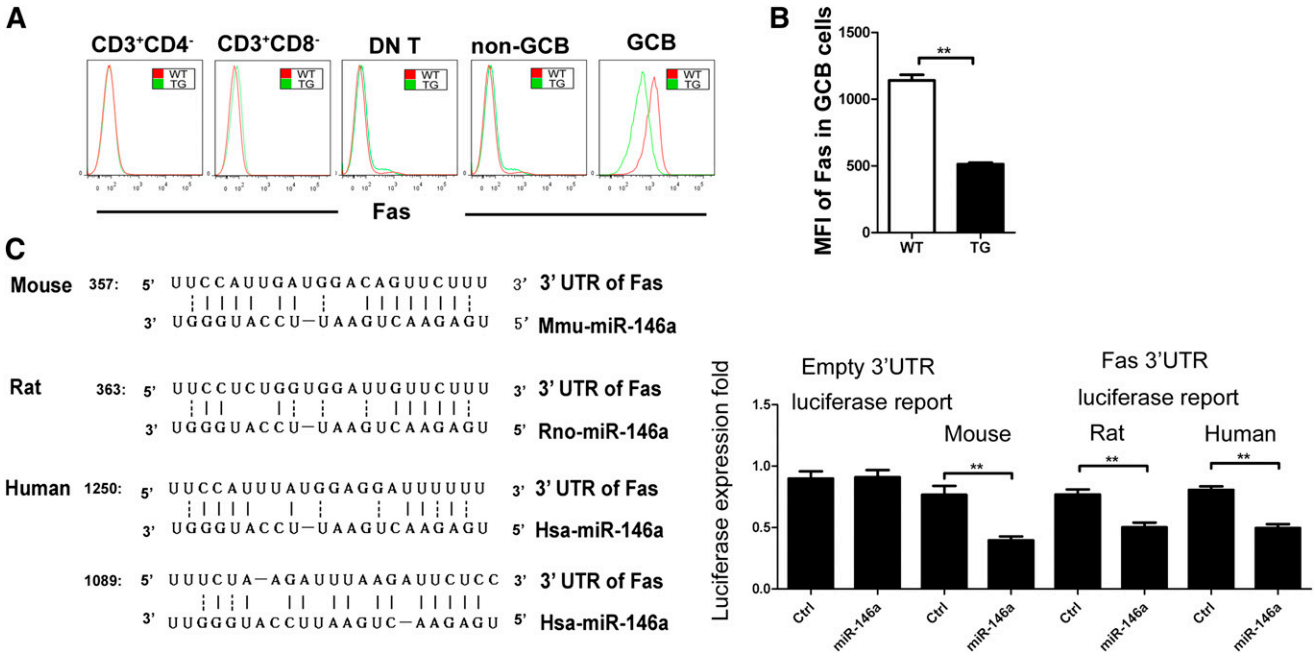

Figure 4. Fas is the direct target of miR-146a in GC B cells. (A) Fas expression in various lymphocyte subsets of lymph nodes from WT and miR-146a TG mice, determined by FACS (gated as $CD3^+CD4^+$, $CD3^+CD8^+$, $CD3^+CD4^-CD8^-TCR\alpha\beta^+$ DN T cells, non-GC B cells [gated as $B220^+PNA^-CD38^{high}$] and GC B cells [gated as $B220^+PNA^+CD38^{low}$]). (B) Fas downregulation in GC B cells (gated as $B220^+PNA^+CD38^{low}$) in dLNs from TG mice. The mean fluorescence intensity (MFI) of the Fas expression detected by FACS was calculated and presented. (C) Putative miR-146a-binding sites in the 3′-UTR of Fas from the rat, mouse, and human. The sequences are partially complementary to each other (left). Cotransfection of 293T cells with the pEZX-Luc vector containing the Fas 3′-UTR (from the rat, mouse, or human) and a plasmid encoding either miR-146a or miR-scramble (Ctrl), and the pEZX-Luc empty vector was also used as a control (bottom). Data are expressed in terms of mean ± standard deviation values. Comparison of means was performed with an unpaired Student 2-tailed *t* test (**$P < .01$).

induce T-cell activation. Moreover, in our in vitro assays, T-cell survival in TG mice was also found to be normal (supplemental Figure 5). An important observation, however, was an abnormal increase in both the cell number and frequency of $CD3^+CD4^-CD8^-TCR\alpha\beta^+$ double-negative (DN) T cells in the spleens of miR-146a TG mice at age 8 to 52 weeks (Figure 2D).

The levels of inflammatory proteins in mouse sera were examined using the Milliplex assay. Although no significant changes were observed in the cytokines and chemokines tested (supplemental Figure 6), higher concentrations of total serum immunoglobulin were observed in miR-146a TG mice; that is, young adult TG mice (at age 8 weeks) had threefold to sixfold higher serum concentrations of total immunoglobulin G1 (IgG1), IgG2b, IgG2a, and IgG3. In aged mice (age 52 weeks), the elevation in IgG1 and IgG2a levels was retained, although at reduced levels (Figure 3A), and no difference was detected in IgM or IgA levels in both 8- and 52-week-old mice (supplemental Figure 7).

Consistent with elevated IgG levels, further analysis showed that the $B220^+$ B-lymphocyte population in lymph nodes was considerably increased (Figure 3B). Furthermore, a similar proportion of B-cell subsets was observed between WT and TG mice, including mature B cells ($B220^+AA4.1^-$) and immature B cells ($B220^+AA4.1^+$), newly formed or activated B cells ($B220^+IgM^+CD21^{low}CD23^{low}$), and follicular B cells ($B220^+IgM^+CD21^{int}CD23^{high}$) (supplemental Figure 8). B-cell development in the bone marrow was also normal in TG mice (supplemental Figure 9). However, with PNA staining, we observed that multiple GC-like structures developed spontaneously in the lymph nodes of TG mice, as early as 8 weeks after birth (Figure 3C). Using the confocal immunofluorescence analysis, similar results with GCs were observed in peripheral lymph nodes of TG mice at age 8 weeks (supplemental Figure 10). Further analysis at the cellular level showed that there was no significant difference in the percentage of Tfh cells between TG and WT mice (supplemental Figure 9). However, in both young adult and aged mice, the fractions and numbers of GC B cells significantly increased in pLNs, mLNs, PPs, and spleens of TG mice (Figure 3D and supplemental Figure 11).

In summary, starting at a young age, miR-146a TG mice developed enlarged spleens and lymph nodes, inflammatory infiltrations in the livers and lungs, increased frequency and numbers of T and B cells, elevated fractions of DN T cells, higher serum IgG levels, and accumulation of GC B cells. These pathological phenotypes remarkably coincided with clinical manifestations of ALPS.

miR-146a specifically targets Fas in GC B cells

Dysfunction of Fas, which leads to interference with the Fas-mediated apoptosis pathway, is generally regarded as a pathogenesis factor in most individuals with ALPS. Therefore, the Fas expression in various lymphocyte populations ($CD3^+CD4^+$ T, $CD3^+CD8^+$ T, $CD3^+CD4^-CD8^-TCR\alpha\beta^+$ DN T, $B220^+PNA^+CD38^{low}$ non-GCB, and $B220^+PNA^-CD38^{high}$ GC B cells) was examined using FACS. As shown previously, the GC B cells were the only cells among these cell populations that had a higher surface density of Fas (Figure 4A-B). Remarkably, the surface Fas level was downregulated in the $B220^+PNA^+CD38^{low}$ population of GC B cells from TG mice (Figure 4B). This downregulation pattern suggests that miR-146a acts as a rheostat rather than a binary off-switch to decrease the Fas expression in GC B cells. The bioinformatics analysis also indicated that Fas could be a direct target of miR-146a (Figure 4C). We tested this hypothesis with a dual luciferase assay. In agreement with a previous report, our results showed that miR-146a overexpression reduced the luciferase activity when cotransfected with plasmids containing the 3′-UTR of Fas (from the mouse,

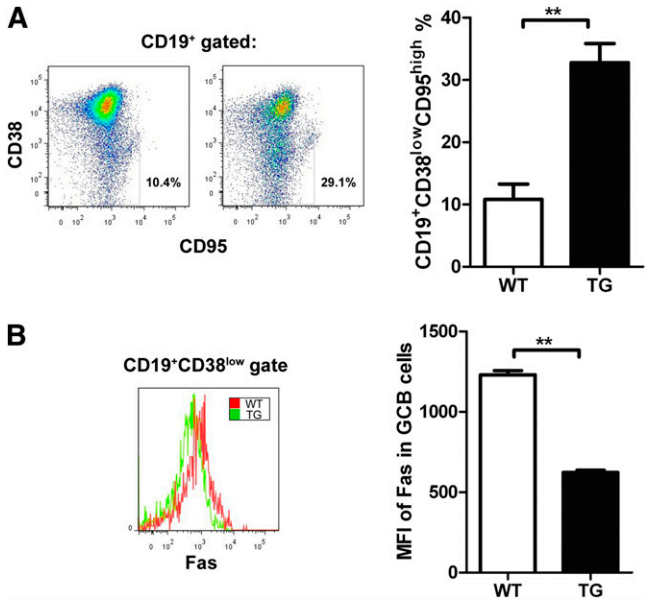

Figure 5. Reproduction of GC B-cell accumulation and Fas downregulation in recipient SCID mice after adoptive transfer of non-GC B cells. Non-GC B cells from miR-146a TG or WT mice were mixed with WT $CD4^+$ T cells at a 1:1 ratio and adoptively transferred into recipient SCID BALB/c mice. (A) Seven days after adoptive transfer, the percentage of $CD19^+CD38^{low}CD95^{high}$ GC B cells was determined by FACS (n = 7). (B) Fas was detected in $CD19^+CD38^{low}$ B cells as described earlier. The mean fluorescence intensity (MFI) of Fas expression was calculated at 3 and 6 days after adoptive transfer. All data are representative of at least 3 independent experiments. All values are expressed in terms of mean ± standard deviation values. Comparison of means was performed with an unpaired Student 2-tailed *t* test (**$P < .01$). The bars indicate standard error of the mean.

rat, or human) in 293T cells (Figure 4C), indicating that Fas is the direct target of miR-146a.[24]

To demonstrate that the suppression of Fas by miR-146a was specifically achieved during the GC formation, rather than originating from the B-cell development process, we mixed non-GC B cells isolated from miR-146a TG or WT with WT $CD4^+$ T cells, followed by adoptive transfer into SCID mice. Seven days after transfer, the Fas expression levels were examined. A significantly higher amount (27% to 42%) of GC B cells was accumulated in transferred B cells from TG mice, compared with those (4% to 16%) from WT animals (Figure 5A). Among the GC B cell population on both the third and seventh day after adoptive transfer, there was a significant reduction in Fas expression on the surface of GC B cells originating from the non-GC B cells of donor TG mice (Figure 5B). However, no significant alteration of Fas was observed in GC B cells from TG mice on either the third or seventh day after adoptive transfer (data not shown). From the third to the seventh day after adoptive transfer, a slight increase of Fas expression was observed in GC B cells of WT mice, which is in agreement with a previous report that the expression of Fas was increased during the GC formation (data not shown). Moreover, these data indicated that miR-146a may be intrinsically required for downregulating Fas during the GC formation.

miR-146a enhances lymphocyte homeostasis expansion

To further elucidate the mechanism underlying miR-146a–mediated B-cell dysfunction, naive B cells were sorted from WT and TG mice, and the gene expression profiles were investigated using the cDNA microarray approach.[25-28] Microarray data were used to assess miR-146a targets with the Sylamer method, which was designed to match the complementation between the seed region of miR-146a and the 3′-UTR of downregulated mRNAs.[29] The analysis showed that the elements capable of pairing to the seed region of miR-146a were significantly enriched in TG B cells (Figure 6A). The previously validated miR-146a targets, such as TRAF6, IRAK1, and CXCR4, were identified in our microarray results (supplemental Figure 12). The functional bioinformatics analysis also suggested that the targets of miR-146a are enriched in the nuclear factor kappa-light chain-enhancer of activated B cells (NF-kB), activator protein 1, interferon regulatory factors, and STAT signaling pathways.[7,10-12] In agreement with the notion that miR-146a targets the NF-κB pathway in a negative feedback manner to regulate macrophage proliferation in response to antigens or mitogens,[7,30] B cells from miR-146a TG mice proliferated to a lesser extent than those from WT mice that were stimulated with LPS (Figure 6B).

Alternatively, the expansion of naive B cells in our TG mouse model could be explained by lymphocyte homeostasis.[31] To test this possibility, B cells isolated from WT and TG mice were adoptively transferred to 6- to 8-week-old recipient SCID mice. Using an EdU-incorporation assay, we found that B cells from TG mice showed hyperhomeostatic proliferation at day 7 after transfer (Figure 6C). Furthermore, adoptive transfer of $CD4^+$ T cells was also performed to investigate T-cell expansion in TG mice. Surprisingly, transferring $CD4^+$ T cells alone from TG mice showed a proliferation rate similar to that for WT mice (Figure 6D). A previous report showed that ablation of Fas specifically in GC B cells impaired the homeostasis of both T and B lymphocytes.[32] Therefore, a combination of T and B cells from the lymph nodes of TG mice was adoptively transferred, and homeostasis proliferation of various subsets gated as $B220^+$, $CD4^+$, and $CD8^+$ was analyzed. Interestingly, T cells from wild-type mice showed hyperhomeostatic proliferation when transferred together with miR-146a TG B cells (Figure 6E). These findings suggested that the sustained expression of miR-146a in B cells is the major factor leading to the enhanced homeostatic expansion of B cells and T cells, which may be an etiologic factor for ALPS-like pathogenesis.

Discussion

We generated miR-146a TG mice that spontaneously develop immunological disorders that resemble the major clinical manifestations of ALPS. The majority of ALPS patients exhibit chronic and nonmalignant lymphadenopathy and splenomegaly with significantly increased numbers of DN T cells and higher serum IgG levels at an early age.[33-37] In addition, ALPS symptoms are typically worse in children but can be relieved in adults to some degree.[35] In miR-146a TG mice, enlarged spleens and lymph nodes were observed at a very early age (3 weeks), and the difference peaked around the fourth week after birth. Elevated levels of DN T cell were also observed in the spleens of all young TG mice. The serum concentrations of IgG1, IgG2b, IgG2a, and IgG3 were threefold to sixfold higher in TG mice at early ages, and the total serum Ig levels at age 52 weeks almost returned to normal levels, except for those of IgG1 and IgG2a. Infiltrative lung lesions and liver dysfunction have been found among 4% to 5% of ALPS patients[38]; similarly, we observed lung and liver infiltration with inflammatory cells in miR-146 TG mice at a much higher incidence rate. Throughout their life, ALPS patients are susceptible to Hodgkin and non-Hodgkin lymphoma; strikingly, we also detected

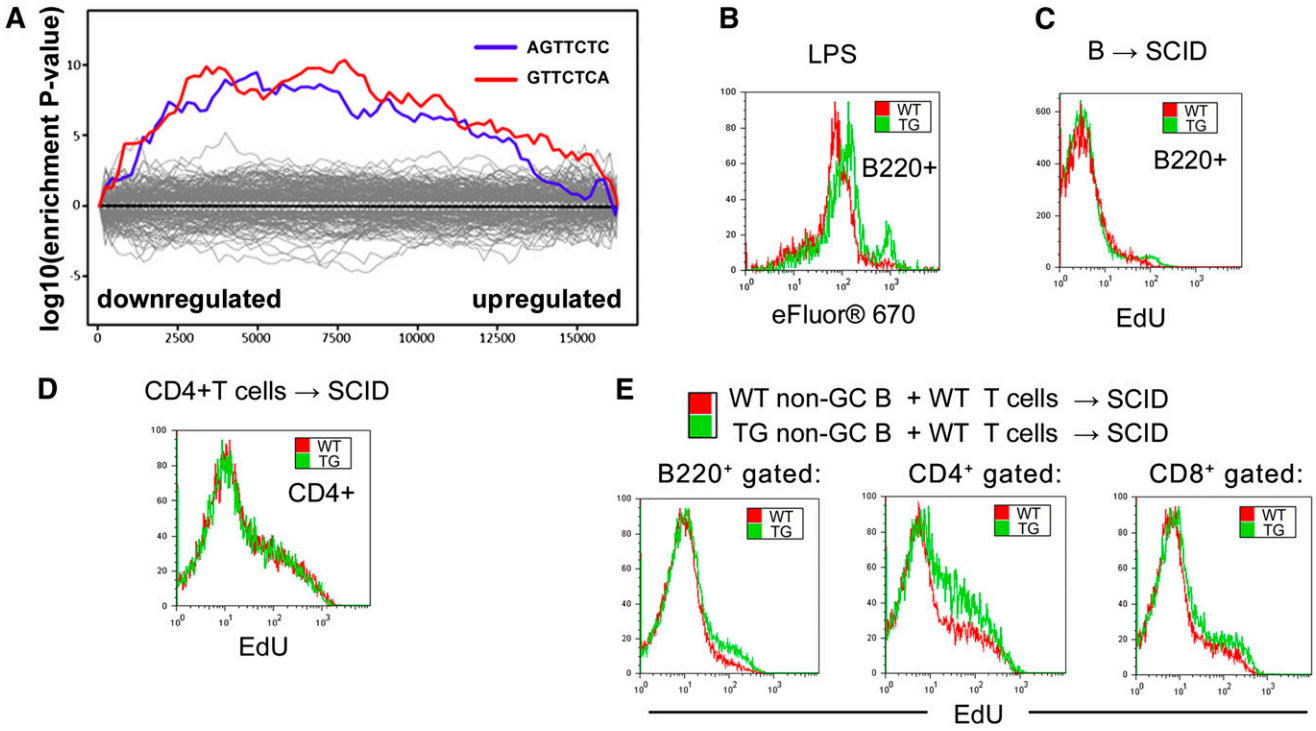

Figure 6. Sylamer enrichment analysis in B cells. (A) The Sylamer enrichment analysis of the miR-146a–binding sites, including AGTTCTC (blue) and GTTCTCA (red) in the 3′-UTRs of differentially expressed genes in B cells. The *x*-axis represents the list of 16 564 identified genes sorted from the most downregulated to the most upregulated ones in the miR-146a–overexpressing B cells. Each 7-mer motif was calculated for its significant enrichment across the 3′-UTRs of genes in the list. These 2 motifs corresponding to the miR-146a seed region are significantly enriched in the downregulated genes. (B) The B cells from WT and miR-146a TG mice were labeled with eFluor670 (an alternative cell proliferation dye of CFSE) and then stimulated with LPS (0.1 μg/mL) in vitro. After 72 hours, cultured cells were collected and analyzed by the CFSE dilution and FACS assays. (C) Non-GC B cells or (D) CD4+ T cells sorted from WT or TG mice and adoptively transferred into SCID mice. After 7 days of adoptive transfer, homeostasis proliferation of non-GC B or CD4+ T cells was detected using the EdU-incorporation assay. (E) Non-GC B cells were sorted from WT or TG mice; naive T cells were sorted from WT mice. T cells were mixed with each type of B cell, and the mixture was adoptively transferred into SCID mice. Seven days post initial transfer, rates of homeostasis proliferation were determined by the Edu-labeling experiments ex vivo. Transferred B cells (Figure 6E, left, including both WT and TG origins) and transferred WT CD4+/CD8+ T cells were examined under the impact of WT B or TG B cells (Figure 6E, middle and right).

a high incidence of lymphoma development in aged miR-146a TG mice (data not shown).

However, there are some significant divergences between our model and ALPS patients. For example, higher serum autoantibody levels are observed among 25% of ALPS patients[34]; despite the accumulation of GC B cells, the levels of anti-dsDNA and anti-ANA in miR-146a TG mice were undetectable (supplemental Figure 13). In addition, during the progress of ALPS in patients, IL-10 significantly increases in circulation and lymphoid tissues. We examined a large panel of cytokines and chemokines in the sera from TG mice and did not find any significant change (supplemental Figure 6). These data imply that overexpression of a single miRNA, miR-146a, in vivo may predominately promote lymphocyte proliferation without fully breaking the threshold for immunological tolerance. This is consistent with the current notion that the full manifestation of ALPS in humans requires accumulation of genetic defects.[37]

Typical ALPS patients inherit genetic defects in the apoptosis pathway, which leads to breakdown of lymphocyte homeostasis and normal immunological tolerance. The major susceptible genes identified include Fas, caspase 10, and Fas ligands.[34,35,37,39,40] Previous reports have shown that Fas mutations in ALPS patients are accompanied by the reduction in Fas protein expression. In this study, we demonstrated that enhanced miR-146a expression results in the downregulation of Fas in GC B cells and eventually leads to the development of major ALPS symptoms. The critical etiologic factor for disease development in our model appears to be the overexpression of miR-146a in naive B cells. Our adaptive transfer experiments clearly showed that TG naive B cells are hyperproliferative, capable of promoting homeostatic proliferation of T cells, and prone to differentiating into GC B cells with reduced surface Fas levels. These findings agree with previous studies showing that the ablation of Fas, specifically in GC B cells but not in T cells, can unbalance the lymphocyte homeostasis and lead to hyperlymphoproliferation.[32] Moreover, downregulated Fas in GC B cells may also promote the survival of activated mature T cells and increase the possibility of losing CD8 or CD4 coreceptor expression on activated mature T cells, thereby leading to the accumulation of DN T cells. In addition, recent studies showed that chronic active Epstein-Barr virus (EBV)–infected patients exhibit clinical ALPS manifestations, including increased DN T cell levels, hepatosplenomegaly, and lymphadenopathy.[39] Interestingly, EBV infection can dramatically induce miR-146a expression in EBV-susceptible B cells.[40,41] Taken together, these findings support the notion that miR-146a may be associated with the development of ALPS and may provide a novel explanation for the pathogenesis of ALPS, especially in cases accompanied by virus infection and chronic inflammation.

High levels of miR-146a are induced in patients with autoimmune disorders, including rheumatoid arthritis, Sjögren's syndrome, and psoriasis, which is in agreement with our observations in TG mice.[16-18] On the other hand, the current conventional wisdom, with its roots in data from miR-146a knockout mice, characterizes miR-146a as an immune suppressor. Ablation of miR-146a in mice results in a spontaneous autoimmune disorder characterized by elevated levels of serum autoantibodies against dsDNA, abnormal activation of

T cells, and increased numbers but impaired suppressor function of Treg cells.[12,42] However, we do not deem these nonreciprocal phenotypes between TG and knockout mice to be necessarily contradictory. Instead, with LPS stimulation, B cells from miR-146a TG mice indeed had lower proliferation rates, which is reciprocal to data from miR-146a–ablated mice. Moreover, TRAF6, IRAK1, and CXCR4 were identified as the major targets in miR-146a–deficient macrophages, and the expression levels of these genes were significantly dampened in our TG naive B cells. Furthermore, the increased miR-146a expression in mice also reduced the frequency of Treg cells, although not to a degree that could result in conventional T-cell activation. Nevertheless, our data demonstrate a novel functional role of miR-146a in facilitating lymphocyte homeostasis proliferation. We hypothesize that the autoimmunity that develops in miR-146a–deficient mice reflects its suppressive effects on the NF-κB pathway, with a dominant function inside innate immune cells, while the ALPS-like symptoms manifested in miR-146a TG mice illustrate its nature in promoting the homeostatic expansion of B cells.

Acknowledgments

The authors especially thank Dr Qijing Li for his advice and suggestions regarding the functional analysis of miR-146a TG mice, as well as for discussing and sharing ideas, and Dr Yu Di for the discussion and suggestions for phenotype analysis, particularly for spontaneous GC formation in TG mice. The authors thank Dr Qiaonan Guo for her help with pathological and immunochemical analyses and Ms Jianhong Mi and Ms Fang Wang for their excellent assistance with immunochemical analysis and cell sorting of lymphocytes via flow cytometry, respectively.

This study was supported by grants from the National Basic Research Program of China (973 program, 2010CB534908 and 2010CB529102), the National Natural Science Foundation of China (30930086, 81273288, and 31028007), the National Science Foundation of Chongqing (2010bb5173), and Youth Innovation Foundation for Third Military Medical University (2010XQN09).

Authorship

Contribution: Y. Wu, Y. Wan, Q.G., Jinjun Zhang, and J.L. designed and performed the study, including the generation of miR-146a TG mice, analysis of the mouse phenotypes, and execution of adoptive transfer experiments. These authors also analyzed and interpreted data and drafted the manuscript; L.Z. performed enzyme-linked immunosorbent assays and isolated the lymphocytes; Jinyu Zhang generated the miR-146a TG mice via microinjection by using lentivirus-based methods; Z.X. performed luciferase assays; X.F. conducted the FACS analysis; S.J. performed Q-PCR and pathological analyses; G.C. performed RNA isolation and microarray assays; Q.J. analyzed the microarray data and performed Sylamer enrichment analysis; and F.L. prepared the cell culture.

Conflict-of-interest disclosure: The authors declare no competing financial interests.

Correspondence: Yuzhang Wu, Institute of Immunology, Third Military Medical University, Gaotangya St 30, Chongqing 400038, China; e-mail: wuyuzhang@yahoo.com; and Ying Wan, Biomedical Analysis Center, Third Military Medical University, Gaotangya St 30, Chongqing 400038, China; e-mail: wanying.cn@gmail.com.

References

1. Bartel DP, Chen CZ. Micromanagers of gene expression: the potentially widespread influence of metazoan microRNAs. *Nat Rev Genet.* 2004; 5(5):396-400.
2. Grosshans H, Filipowicz W. Proteomics joins the search for microRNA targets. *Cell.* 2008;134(4): 560-562.
3. Ambros V. The functions of animal microRNAs. *Nature.* 2004;431(7006):350-355.
4. Baltimore D, Boldin MP, O'Connell RM, Rao DS, Taganov KD. MicroRNAs: new regulators of immune cell development and function. *Nat Immunol.* 2008;9(8):839-845.
5. Lindsay MA. microRNAs and the immune response. *Trends Immunol.* 2008;29(7):343-351.
6. Tsitsiou E, Lindsay MA. microRNAs and the immune response. *Curr Opin Pharmacol.* 2009; 9(4):514-520.
7. Taganov KD, Boldin MP, Chang KJ, Baltimore D. NF-kappaB-dependent induction of microRNA miR-146, an inhibitor targeted to signaling proteins of innate immune responses. *Proc Natl Acad Sci USA.* 2006;103(33):12481-12486.
8. Perry MM, Moschos SA, Williams AE, Shepherd NJ, Larner-Svensson HM, Lindsay MA. Rapid changes in microRNA-146a expression negatively regulate the IL-1beta-induced inflammatory response in human lung alveolar epithelial cells. *J Immunol.* 2008;180(8):5689-5698.
9. Rom S, Rom I, Passiatore G, et al. CCL8/MCP-2 is a target for mir-146a in HIV-1-infected human microglial cells. *FASEB J.* 2010;24(7):2292-2300.
10. Hou J, Wang P, Lin L, et al. MicroRNA-146a feedback inhibits RIG-I-dependent Type I IFN production in macrophages by targeting TRAF6, IRAK1, and IRAK2. *J Immunol.* 2009;183(3): 2150-2158.
11. Curtale G, Citarella F, Carissimi C, et al. An emerging player in the adaptive immune response: microRNA-146a is a modulator of IL-2 expression and activation-induced cell death in T lymphocytes. *Blood.* 2010;115(2):265-273.
12. Lu LF, Boldin MP, Chaudhry A, et al. Function of miR-146a in controlling Treg cell-mediated regulation of Th1 responses. *Cell.* 2010;142(6): 914-929.
13. Kuchen S, Resch W, Yamane A, et al. Regulation of microRNA expression and abundance during lymphopoiesis. *Immunity.* 2010;32(6):828-839.
14. Li J, Wan Y, Guo Q, et al. Altered microRNA expression profile with miR-146a upregulation in CD4+ T cells from patients with rheumatoid arthritis. *Arthritis Res Ther.* 2010;12(3):R81.
15. Pauley KM, Satoh M, Chan AL, Bubb MR, Reeves WH, Chan EK. Upregulated miR-146a expression in peripheral blood mononuclear cells from rheumatoid arthritis patients. *Arthritis Res Ther.* 2008;10(4):R101.
16. Nakasa T, Miyaki S, Okubo A, Hashimoto M, Nishida K, Ochi M, Asahara H. Expression of microRNA-146 in rheumatoid arthritis synovial tissue. *Arthritis Rheum.* 2008;58(5):1284-1292.
17. Stanczyk J, Pedrioli DM, Brentano F, et al. Altered expression of MicroRNA in synovial fibroblasts and synovial tissue in rheumatoid arthritis. *Arthritis Rheum.* 2008;58(4):1001-1009.
18. Sonkoly E, Wei T, Janson PC, et al. MicroRNAs: novel regulators involved in the pathogenesis of psoriasis? *PLoS ONE.* 2007;2(7):e610.
19. Alevizos I, Illei GG. MicroRNAs in Sjögren's syndrome as a prototypic autoimmune disease. *Autoimmun Rev.* 2010;9(9):618-621.
20. Jazdzewski K, Murray EL, Franssila K, Jarzab B, Schoenberg DR, de la Chapelle A. Common SNP in pre-miR-146a decreases mature miR expression and predisposes to papillary thyroid carcinoma. *Proc Natl Acad Sci USA.* 2008; 105(20):7269-7274.
21. He H, Jazdzewski K, Li W, et al. The role of microRNA genes in papillary thyroid carcinoma. *Proc Natl Acad Sci USA.* 2005;102(52): 19075-19080.
22. Lois C, Hong EJ, Pease S, Brown EJ, Baltimore D. Germline transmission and tissue-specific expression of transgenes delivered by lentiviral vectors. *Science.* 2002;295(5556):868-872.
23. Livak KJ, Schmittgen TD. Analysis of relative gene expression data using real-time quantitative PCR and the 2(-Delta Delta C(T)) Method. *Methods.* 2001;25(4):402-408.
24. Suzuki Y, Kim HW, Ashraf M, Haider HK. Diazoxide potentiates mesenchymal stem cell survival via NF-kappaB-dependent miR-146a expression by targeting Fas. *Am J Physiol Heart Circ Physiol.* 2010;299(4):H1077-H1082.
25. Farh KK, Grimson A, Jan C, et al. The widespread impact of mammalian MicroRNAs on mRNA repression and evolution. *Science.* 2005; 310(5755):1817-1821.
26. Giraldez AJ, Mishima Y, Rihel J, et al. Zebrafish MiR-430 promotes deadenylation and clearance of maternal mRNAs. *Science.* 2006;312(5770):75-79.

27. Rodriguez A, Vigorito E, Clare S, et al. Requirement of bic/microRNA-155 for normal immune function. *Science.* 2007;316(5824):608-611.

28. Guo H, Ingolia NT, Weissman JS, Bartel DP. Mammalian microRNAs predominantly act to decrease target mRNA levels. *Nature.* 2010; 466(7308):835-840.

29. van Dongen S, Abreu-Goodger C, Enright AJ. Detecting microRNA binding and siRNA off-target effects from expression data. *Nat Methods.* 2008; 5(12):1023-1025.

30. Zhao JL, Rao DS, Boldin MP, Taganov KD, O'Connell RM, Baltimore D. NF-kappaB dysregulation in microRNA-146a-deficient mice drives the development of myeloid malignancies. *Proc Natl Acad Sci USA.* 2011;108(22):9184-9189.

31. Cabatingan MS, Schmidt MR, Sen R, Woodland RT. Naive B lymphocytes undergo homeostatic proliferation in response to B cell deficit. *J Immunol.* 2002;169(12):6795-6805.

32. Hao Z, Duncan GS, Seagal J, et al. Fas receptor expression in germinal-center B cells is essential for T and B lymphocyte homeostasis. *Immunity.* 2008; 29(4):615-627.

33. Sneller MC, Straus SE, Jaffe ES, Jaffe JS, Fleisher TA, Stetler-Stevenson M, Strober W. A novel lymphoproliferative/autoimmune syndrome resembling murine lpr/gld disease. *J Clin Invest.* 1992;90(2):334-341.

34. Fisher GH, Rosenberg FJ, Straus SE, et al. Dominant interfering Fas gene mutations impair apoptosis in a human autoimmune lymphoproliferative syndrome. *Cell.* 1995;81(6):935-946.

35. Bettinardi A, Brugnoni D, Quirós-Roldan E, Malagoli A, La Grutta S, Correra A, Notarangelo LD. Missense mutations in the Fas gene resulting in autoimmune lymphoproliferative syndrome: a molecular and immunological analysis. *Blood.* 1997;89(3):902-909.

36. Lenardo MJ, Oliveira JB, Zheng L, Rao VK. ALPS-ten lessons from an international workshop on a genetic disease of apoptosis. *Immunity.* 2010;32(3):291-295.

37. Magerus-Chatinet A, Neven B, Stolzenberg MC, et al. Onset of autoimmune lymphoproliferative syndrome (ALPS) in humans as a consequence of genetic defect accumulation. *J Clin Invest.* 2011;121(1):106-112.

38. Rao VK, Straus SE. Causes and consequences of the autoimmune lymphoproliferative syndrome. *Hematology.* 2006;11(1):15-23.

39. Nomura K, Kanegane H, Otsubo K, Wakiguchi H, Noda Y, Kasahara Y, Miyawaki T. Autoimmune lymphoproliferative syndrome mimicking chronic active Epstein-Barr virus infection. *Int J Hematol.* 2011;93(6):760-764.

40. Motsch N, Pfuhl T, Mrazek J, Barth S, Grässer FA. Epstein-Barr virus-encoded latent membrane protein 1 (LMP1) induces the expression of the cellular microRNA miR-146a. *RNA Biol.* 2007; 4(3):131-137.

41. Cameron JE, Yin Q, Fewell C, et al. Epstein-Barr virus latent membrane protein 1 induces cellular MicroRNA miR-146a, a modulator of lymphocyte signaling pathways. *J Virol.* 2008;82(4): 1946-1958.

42. Boldin MP, Taganov KD, Rao DS, et al. miR-146a is a significant brake on autoimmunity, myeloproliferation, and cancer in mice. *J Exp Med.* 2011;208(6): 1189-1201.